

Article

Copper Oxide Nanoparticles Synthesized from *Indigofera linnaei* Ali and This Plant's Biological Applications

Nadarajan Prathap ¹, Nagarajan Dravid ¹, Srinivasan R. Kaarmukhilnilavan ² ,
Muthugounder Subaramanian Shivakumar ³, Srinivasan Venkatesan ^{1,*}, Mohammed Rafi Shaik ^{4,*} 
and Baji Shaik ⁵

¹ Department of Environmental Science, School of Energy and Environmental Sciences, Periyar University, Salem, Tamil Nadu, India

² Sona College of Arts and Science, Salem, Tamil Nadu, India

³ Department of Biotechnology, School of Biosciences, Periyar University, Salem, Tamil Nadu, India

⁴ Department of Chemistry, College of Science, King Saud University, P.O. Box 2455, Riyadh 11451, Saudi Arabia

⁵ School of Chemical Engineering, Yeungnam University, Gyeongsan 38541, Republic of Korea

* Correspondence: svenkatesan75@gmail.com (S.V.); mrshaik@ksu.edu.sa (M.R.S.);
Tel.: +966-11-4670439 (M.R.S.)

Abstract: The leaf extract of *Indigofera linnaei* Ali, an Indian medicinal plant, was utilized in the synthesis of copper oxide nanoparticles (CuO-NPs). Green chemistry is a safe and cost-effective method for the synthesis of nanoparticles using plant extracts. The synthesis of CuO NPs was confirmed using ultraviolet–visible (UV-visible) spectrum λ -max data with two peaks at 269 and 337 nm. Different functional groups were identified using Fourier-transform infrared spectroscopy (FT-IR). X-ray diffraction (XRD) was used to confirm the crystalline structure of the CuO-nanoparticles. Scanning electron microscopy (SEM) and energy dispersive X-ray (EDX) analyses were performed to examine the surface morphology and elemental composition of the biosynthesized CuO-NPs. Furthermore, the synthesized CuO-NPs exhibited antibacterial activity against *Staphylococcus aureus*, *Pseudomonas aeruginosa*, *Escherichia coli*, and *Enterococcus faecalis*. Additionally, they exhibited a good insecticidal effect on *Culex quinquefasciatus* larvae, with low LC₅₀ 55.716 μ g/mL and LC₉₀ 123.657 μ g/mL values. The CuO-NPs inhibited human breast cancer cells in a concentration-dependent manner, with an IC₅₀ value of 63.13 μ g/mL.

Keywords: *Indigofera linnaei* Ali; copper oxide nanoparticles; antibacterial; anticancer larvicidal activity



Citation: Prathap, N.; Dravid, N.; Kaarmukhilnilavan, S.R.; Shivakumar, M.S.; Venkatesan, S.; Shaik, M.R.; Shaik, B. Copper Oxide Nanoparticles Synthesized from *Indigofera linnaei* Ali and This Plant's Biological Applications. *Inorganics* **2023**, *11*, 462. <https://doi.org/10.3390/inorganics11120462>

Academic Editor: Carlos Martínez-Boubeta

Received: 2 October 2023

Revised: 17 November 2023

Accepted: 22 November 2023

Published: 28 November 2023



Copyright: © 2023 by the authors. Licensee MDPI, Basel, Switzerland. This article is an open access article distributed under the terms and conditions of the Creative Commons Attribution (CC BY) license (<https://creativecommons.org/licenses/by/4.0/>).

1. Introduction

Nanotechnology is a transformative frontier in science and engineering that harnesses the unique attributes of nanoscale materials to create innovative solutions across multiple fields [1]. One of the most promising advancements in this field is the synthesis and application of nanomaterials, which, owing to their amplified surface area, stability, and conductivity, have diverse applications, ranging from engineering to biomedical instrumentation [2]. The potential hazards associated with chemical synthesis methods, coupled with increasing environmental concerns, have shifted the focus towards green and sustainable approaches to nanoparticle synthesis.

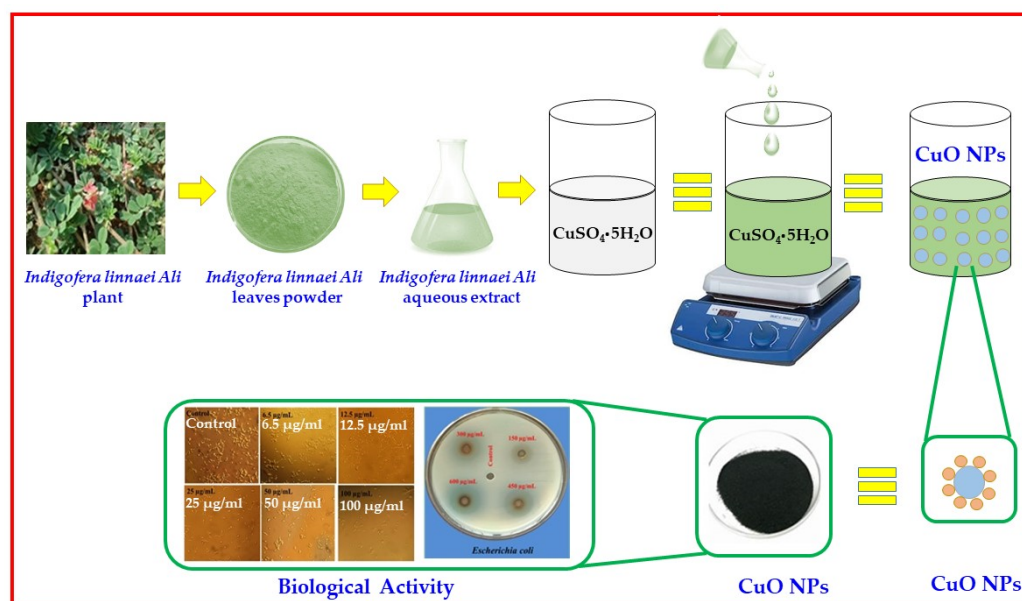
The use of biological materials, particularly plant extracts and microorganisms, presents a compelling case for developing ecofriendly, cost-effective, and safe alternatives [3,4]. Biological synthesis can be carried out using plant parts, secondary metabolites from plants (leaf, root, stem, fruit, and flower secondary metabolites), and microbes and their secondary metabolites [5]. In recent years, metals such as copper (Cu), silver (Ag), zinc (Zn), iron (Fe), gold (Au), silicon (Si), nickel (Ni), and platinum (Pt) have been used in the green synthesis of nanoparticles for biomedical applications [6]. The potential hazards associated with

chemical synthesis methods, coupled with increasing environmental concerns, have shifted the focus towards green and sustainable approaches to nanoparticle synthesis. This biological synthesis not only eliminates the need for toxic chemicals, high temperatures, and sophisticated instrumentation but also leverages the intrinsic bioactive compounds present in these natural resources to enhance the miniaturization and stabilization of nanoparticles. Copper (Cu) is an essential nutrient for plant growth, enzymes, photosynthesis, and RNA synthesis [7]. With regard to trade, Cu nanoparticles are extensively used to produce antimicrobial, larvicidal, anticancer, and antioxidant products [8]. Plants such as *Caesalpinia bonducella* [9], *Punica granatum* [10], *Ocimum sanctum* [11], *Saussurea lappa* [12], and *Ziziphus spina-christi* [13] have been used for the synthesis of copper nanoparticles (CuO NPs). The synthesis of CuO NPs using plant extracts appears to be a favorable and environmentally friendly approach in the field of nanotechnology [14]. CuO NPs exhibit exceptional properties and a wide range of applications in numerous scientific and industrial domains, such as catalysis, electronics, energy storage, and biomedicine [15]. In recent years, the use of plant extracts as reducing and stabilizing agents for the green synthesis of nanoparticles has gained considerable attention due to its sustainable and eco-friendly nature [16].

Traditional methods of producing CuO nanoparticles frequently comprise the use of hazardous chemicals, high temperatures, and energy-intensive processes, which can have adverse environmental and health impacts [17]. In contrast, green synthesis methods employ natural plant extracts rich in bioactive compounds, such as phytochemicals, polyphenols, and flavonoids, to enable the size reduction and stabilization of CuO NPs. These plant-derived compounds act as both reducing and capping agents, making the corresponding synthesis method not only more sustainable but also safer for investigators and the environment [18]. The green synthesis of CuO NPs using plant extracts offers numerous advantages, comprising reduced environmental pollution, lower energy consumption, cost-effectiveness, and the potential for large-scale production. Additionally, the use of plant extracts adds a new dimension to nanoparticle synthesis, as different plant species and their extracts may convey exceptional properties and functionalities to the resulting CuO nanoparticles [19].

We hypothesize that CuO NPs hold vast potential for a wide range of biological applications. Additionally, the antimicrobial properties of CuO NPs suggest their effectiveness in combatting drug-resistant infections and designing supportive novel therapeutic approaches. We also assume that the controlled functionalization of CuO NPs will permit personalized solutions for precise biological challenges, further enhancing their potential impact on healthcare and life sciences. Through inclusive examination and investigation, we aimed to authenticate our hypothesis and enhance the growing body of knowledge concerning the usage of CuO NPs for biological applications. Our research will not only advance the understanding of these nanoparticles but also enable the development of innovative strategies that may eventually lead to improved patient care, more effective treatments, and enhanced diagnostic techniques in the realm of life sciences. *Indigofera linnaei* Ali is an annual herb with small trailing branches belonging to the Fabaceae family. It is dispersed throughout India, China, Nepal, Pakistan, Sri Lanka, and Australia, where it is used as an indigenous medicine to treat tumors, liver inflammation, arthritis, and rheumatism [20,21]. The juice of *I. linnaei* Ali is known for its diuretic and antiscorbutic properties [22]. In the current study, we applied the medicinal plant *Indigofera linnaei* Ali as both a bioreductant and stabilizing agent for the green synthesis of CuO NPs. *Indigofera linnaei* Ali possesses a rich content of phytochemicals such as glycosides, terpenoids, alkaloids, and flavonoids, which greatly support its feasible reducing ability. Hence, the leaf extract of *I. linnaei* Ali can be utilized for the synthesis of CuO NPs. The green-synthesized CuO NPs (Scheme 1) were characterized via several characterization techniques, such as UV-visible spectroscopy, FT-IR, XRD, SEM, EDX, etc. Moreover, the potential antimicrobial properties of the as-synthesized CuO NPs were evaluated against various bacterial strains, such as *Escherichia coli*, *Pseudomonas aeruginosa*, *Enterococcus faecalis*, and *Staphylococcus aureus*. The as-synthesized CuO nanoparticles are effective against the larvae of the mosquito *Culex*

quinquefasciatus, and the cytotoxicity studies exposed the anticancer properties of the CuO NPs by revealing their outstanding growth rate inhibition in MCF-7 cancer cells.



Scheme 1. Graphical representation of green synthesis of CuO NPs using *Indigofera linnaei* Ali plant extract and its biological activity.

2. Results

2.1. UV-Visible Spectrum Analysis

The CuO-NP-synthesized solution exhibited characteristic absorption peaks in the 200–700 nm wavelength range. Two prominent absorption peaks were observed at 269 and 337 nm (Figure 1). These peaks can be attributed to the Surface Plasmon Resonance (SPR) of Cu-NPs. The manifestation of the SPR band was a clear indication of the concentration of phytochemical reducing agents as well as the size and morphology of the nanoparticles. Additionally, the absorption peaks detected at 243 and 340 nm can be correlated with the core electrons of the copper within the Cu-NPs, as reported in a previous study [23]. Similarly, the CuO-NPs produced using an aqueous extract of *Cardiospermum halicacabum* leaves revealed absorption peaks at 264 and 333 nm. The synthesis of these nanoparticles is fascinating. The generated OH ions, which were derived from water molecules, interacted with copper sulfate, resulting in the formation of copper hydroxides. Subsequently, the decomposition of this nanoparticle conjugate ensued, eventually leading to the production of CuO-NPs [24]. The absorption peaks and patterns identified in our study are consistent with the findings of previous reports [25–27]. The similarities in the peak wavelengths provided consistent evidence regarding the properties and behavior of the CuO-NPs.

2.2. FT-IR Analysis

Fourier-transform infrared spectroscopy (FT-IR) was employed to analyze the functional groups of the plant metabolites present in the aqueous extract of *I. linnaei* Ali plants as well as to identify the functional groups present on the surfaces of the Cu-NPs. In the FT-IR spectra, pronounced peaks were detected at wavenumbers such as 3142, 2976, 2882, 1615, 1394, 1058, 803, 660, and 587 cm^{-1} (Figure 2). The absorption peak at 3142 cm^{-1} represents the N-H stretching of amines. The peak at 2976 represents -OH stretching vibrations, and the weak band at 2882 cm^{-1} can be assigned to -OH bending vibrations. The peak at 1058 cm^{-1} indicated strong C-O stretching. The other small, weak peaks at 1394 and 1615 cm^{-1} may indicate the presence of C=C and C=O bending vibration modes. A weak peak was observed at 660 cm^{-1} in the band that arose from the Cu-O stretching vibration, while similar peaks at 587 cm^{-1} and 803 cm^{-1} are associated with the vibration of C-H

groups [28]. According to the FT-IR results, acids, polyphenols, proteins, alkaloids, and carboxylic acid functional groups could be found in the Cu-NPs [29].

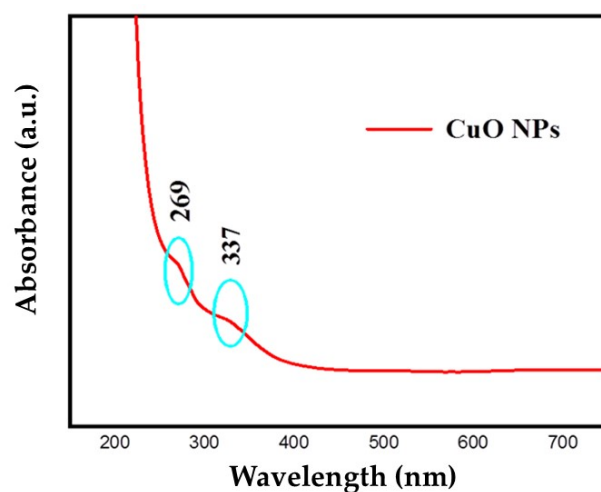


Figure 1. UV-Vis spectrum results of CuO NPs.

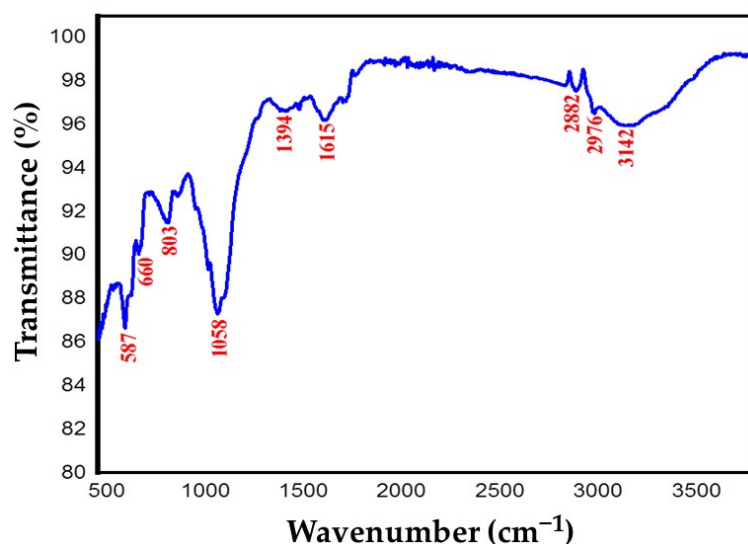


Figure 2. FTIR spectrum of biosynthesized CuO-NPs.

2.3. XRD Analysis

The synthesis of the CuO NPs was confirmed via X-ray diffraction (XRD) analysis. The crystal size of the nanoparticles was 113 nm. The average crystalline structure size of the biosynthesized CuO NPs was calculated using Debye Scherrer's equation [30], where k denotes the shape constant of the geometric factor (0.9), λ represents wavelength, β is the line broadening at half-maximum intensity, θ is the Bragg angle, and D is the average crystalline size of the nanoparticles. As shown in Figure 3, the major XRD 2θ value peaks of the biosynthesized CuO-NPs that appeared at 28.50, 25.90, 26.05, 28.49, 36.15, 39.98, 43.5, 44.97, 47.53, 50.31, 55.19, and 59 were ascribed to (002), (021), (021), (111), (002), (111), (200), (220), (-202), (200), (-311), and (202) miller index planes. The sharp peak at $2\theta = 38.7$ with the diffraction of the (111) plane corresponds to CuO NPs, indicating that the synthesized CuO NPs are crystalline and monoclinic in nature [9,31].

These unidentified peaks appeared because of the deposition of photo-molecules on the surfaces of the CuO-NPs during synthesis [32].

$$D = k\lambda/\beta \frac{1}{2} \cos \theta \quad (1)$$

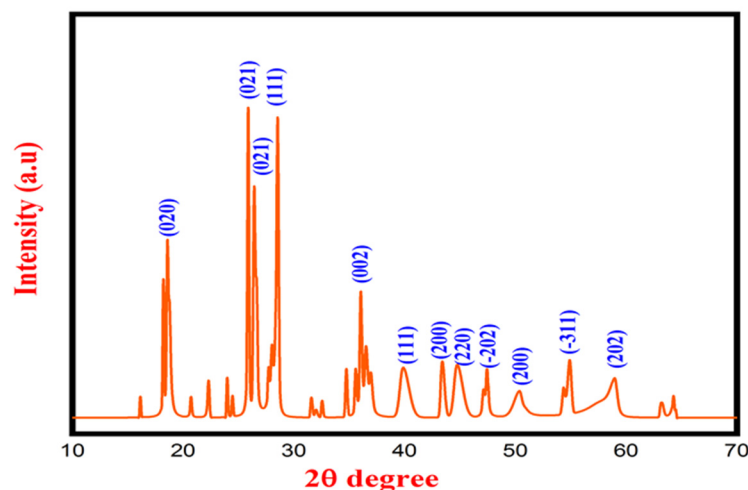


Figure 3. XRD analysis of CuO-NPs.

2.4. SEM and EDX Analysis

Scanning electron microscopy (SEM) was used to assess the surface morphology of the biosynthesized CuO-NPs. The SEM images depicted in Figure 4a,b offer various resolutions, providing a detailed view of the CuO-NPs. Notably, these images reveal a mix of spherical and cuboidal morphologies, albeit with some degree of agglomeration, which is not uncommon in nanoparticle synthesis and can be attributed to various factors, such as high surface energy. Further insights into the composition of the nanoparticles were obtained using energy dispersive X-ray (EDX) spectroscopy. Figure 5a,b show the EDX spectra of the CuO-NPs. Dominantly, copper presented a substantial peak, accounting for 29.40% of the elemental composition. Additionally, carbon and oxygen were recorded to constitute 19.45% and 51.15%, respectively. The presence of carbon and oxygen is suggestive of organic molecules on the nanoparticle surface, likely stemming from phytochemicals in the green synthesis process. Phytochemicals have been postulated to function as both reducing and capping agents, facilitating the formation and stabilization of CuO-NPs [10].

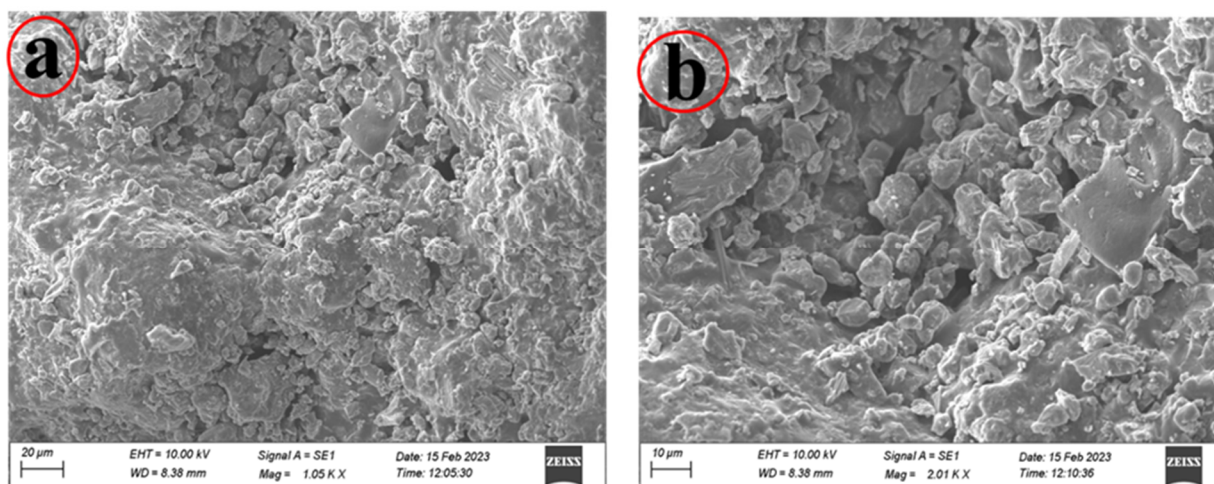


Figure 4. SEM images of biosynthesized CuO-NPs: (a) 20 μm and (b) 10 μm.

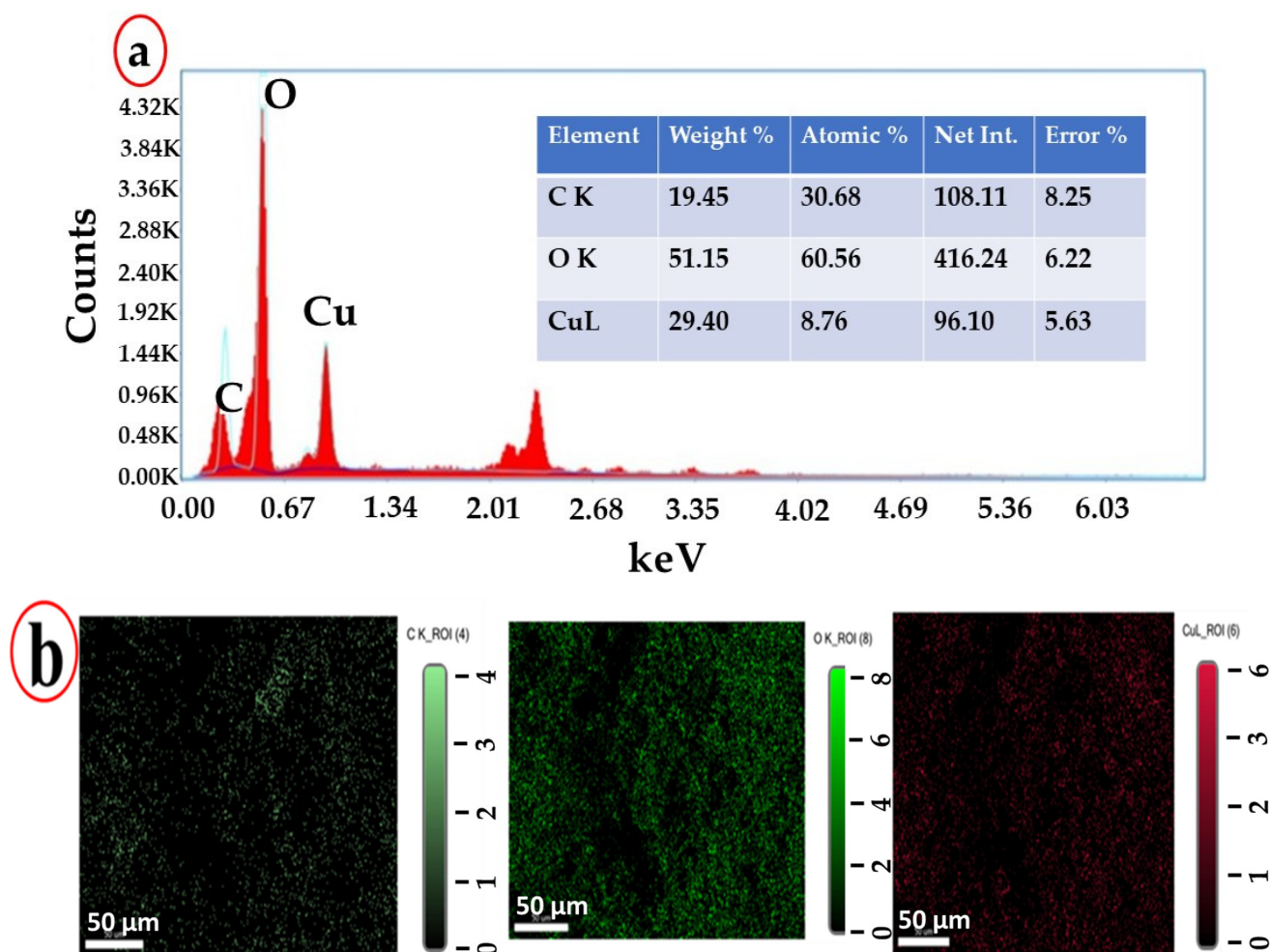


Figure 5. (a) EDX spectrum of biosynthesized CuO-NPs and (b) elemental mapping analysis of CuO-NPs.

Furthermore, the significant presence of copper confirms the successful synthesis of CuO-NPs, whereas the elevated oxygen level aligns with the oxidized nature of the nanoparticles. The detection of carbon signals, possibly associated with plant-derived compounds, aligns with prior research, where phytochemicals were implicated in nanoparticle synthesis, playing pivotal roles in reduction, stabilization, and capping. Collectively, these results underscore the intricate and multifaceted roles of phytochemicals in the green synthesis of CuO-NPs.

2.5. Antibacterial Activity

The biosynthesized CuO-NPs exhibited pronounced antibacterial efficacy against a range of bacterial pathogens. Significant zones of inhibition were observed for pathogens such as *Staphylococcus aureus*, *Enterococcus faecalis*, *Escherichia coli*, and *Pseudomonas aeruginosa*, as shown in Figure 6a [28]. In contrast, dimethyl sulfoxide (DMSO) was used as a negative control and did not demonstrate any inhibitory activity against bacterial cells, thereby underscoring the antibacterial ability of CuO-NPs [29].

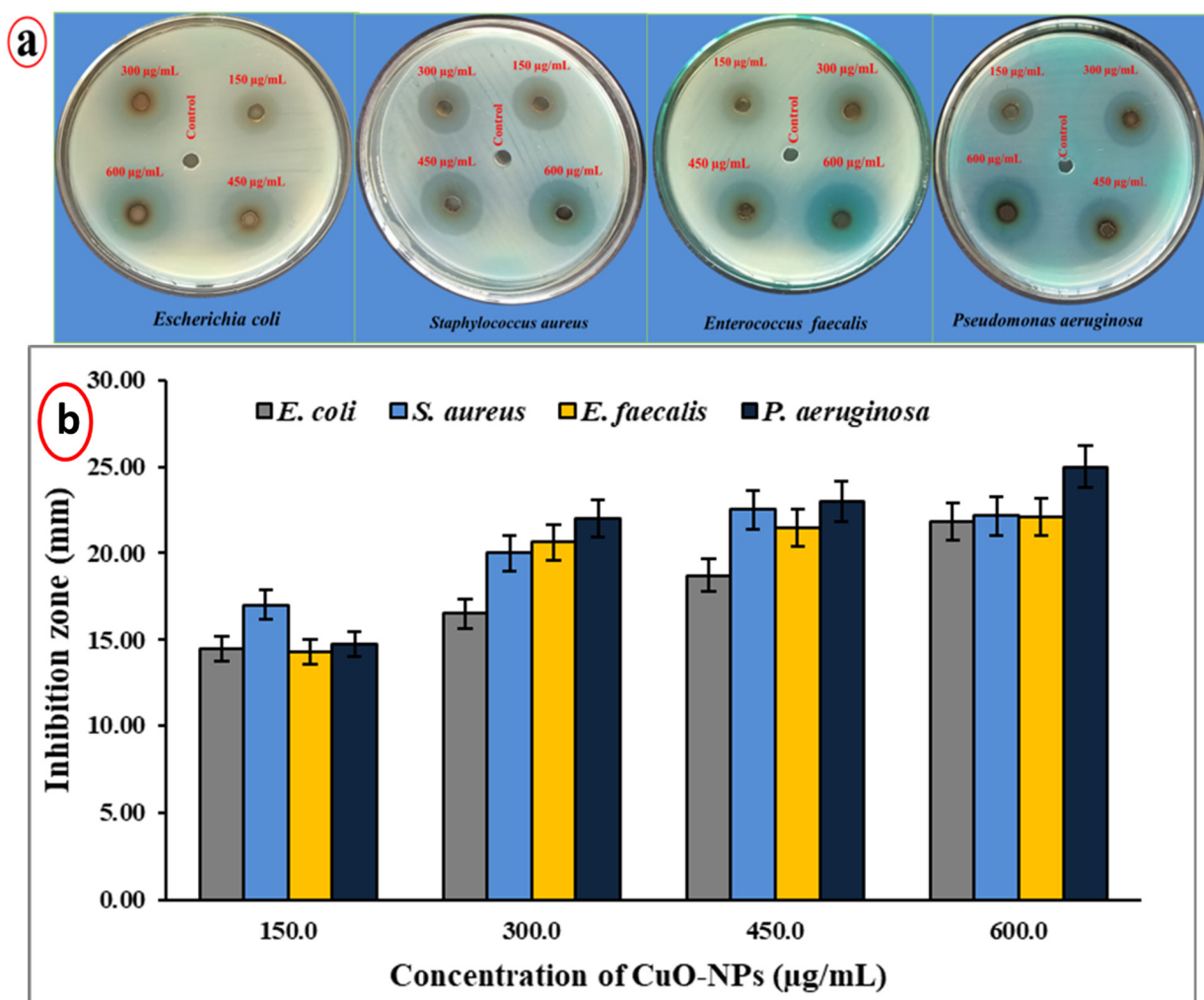


Figure 6. (a) Antibacterial activity of CuO-NPs exerted via agar well diffusion and (b) zone of inhibition with bacterial pathogens.

A prominent mechanism through which CuO-NPs exert their antibacterial action is believed to be their interaction with bacterial cells, primarily occurring via the thiol groups present in bacterial proteins. This interaction synergistically amplifies the inherent antibacterial properties of CuO-NPs. Moreover, a concentration-dependent trend was observed, where the zone of inhibition expanded with increasing doses of CuO-NPs, suggesting a dose-dependent relationship between their antibacterial efficacies (Figure 6). In the broader spectrum of nanoparticle research, metal oxide nanoparticles such as CuO-NPs have been spotlighted for their potential in antimicrobial applications. Their mode of action, which involves the disruption of bacterial cell membranes or interference with essential cellular processes, provides an avenue for potential therapeutic applications, especially in an era in which antibiotic resistance is a rising concern [33,34].

2.6. Assay for the Determination of Minimum Inhibitory Concentration (MIC)

The antimicrobial potency of the biosynthesized CuO-NPs was evaluated across varying concentrations, namely, 150.0, 300.0, 450.0, and 600.0 µg/mL, to establish the minimum inhibitory concentration (MIC) values. As shown in Figure 7, as the concentration of CuO-NPs increased, there was an associated decrease in microbial growth. Specifically, the MIC value for *Pseudomonas aeruginosa* was determined to be 450.0 µg/mL.

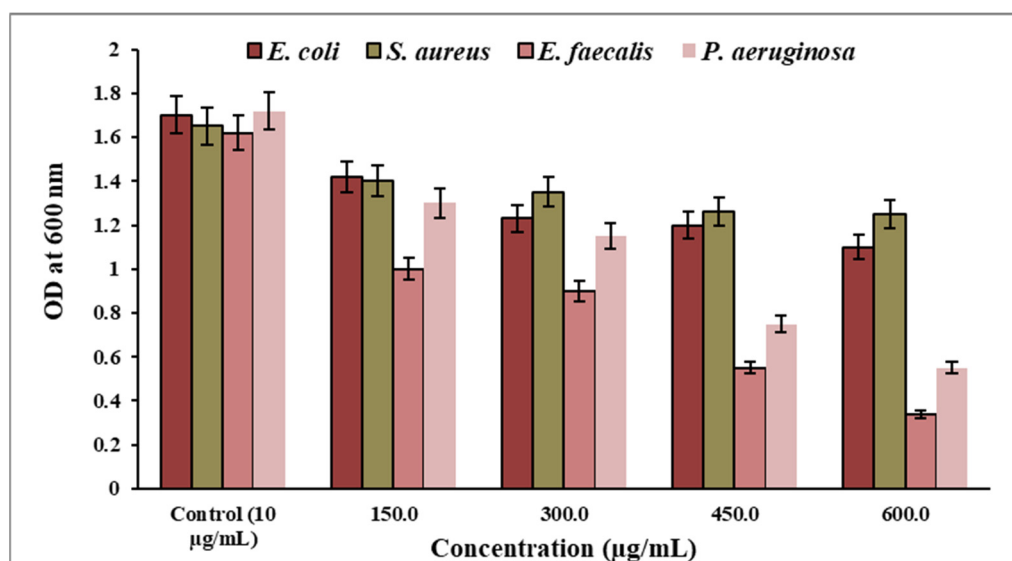


Figure 7. MIC values of CuO-NPs against bacterial pathogens.

In the current study, the Gram-positive bacteria demonstrated lower susceptibility to the biosynthesized CuO-NPs than their Gram-negative counterparts. This differential antibacterial activity can be attributed to electrostatic interactions between the bacterial cell membrane and the copper ions emanating from the nanoparticles. Given that peptidoglycans in bacterial cell walls are intrinsically negatively charged, they are naturally drawn to positively charged Cu^{2+} ions, especially when CuO-NPs are dispersed in a liquid growth medium [35]. To further elucidate the heightened antimicrobial efficacy observed, it was hypothesized that the negative charges of bacterial cell membranes are destabilized by positively charged copper ions. This interaction facilitates the release of nanoparticles into bacterial cells, culminating in protein denaturation and eventual bacterial cell death [36].

2.7. Larvicidal Activity

This section reveals the larvicidal efficacy of the biosynthesized CuO-NPs against the fourth-instar larvae of *Culex quinquefasciatus*. A marked mortality rate was observed with LC_{50} and LC_{90} values of 55.0 and 123.0 $\mu\text{g}/\text{mL}$, respectively, as shown in Table 1. In a related study by Vinothkanna et al. [37], CuO-NPs biosynthesized from *Rubia cordifolia* bark extract exhibited a 72% larvicidal effect against *Culex quinquefasciatus* larvae, further pointing toward the potent larvicidal capabilities of CuO-NPs. Based on these results, it was postulated that the mechanism underlying this lethal effect on mosquito larvae stems from the ability of nanoparticles to permeate the larval body. Once inside, these nanoparticles demolish the cellular structures, targeting enzymes and organelles. This interference leads to the destruction of cellular pathways and cell death [38,39].

Table 1. Larvicidal activity of aqueous extract of *I. linnaei* Ali-synthesized CuO-NPs against *Culex quinquefasciatus*.

Insect	Con. (µg/mL)	Mortality (%)	LC ₅₀ (LCL-UCL) * (µg/mL)	LC ₉₀ (LCL-UCL) (µg/mL)	χ ²	df
<i>C. quinquefasciatus</i>	Control	00.00 ± 00	55.716 (50.200–61.710)	123.657 (104.960–156.663)	11.587	13
	20	10.00 ± 1.00				
	40	21.66 ± 0.57				
	60	48.33 ± 0.57				
	80	71.66 ± 0.57				
	100	90.00 ± 1.00				

* LCL—lower control limit, UCL—upper control limit, and df—degrees of freedom.

2.8. Anticancer Activity

For comparison, previous research involving CuO-NPs synthesized from *Dillenia indica* ethanol leaf extract was reviewed. These nanoparticles, characterized by an average size of 5 nm, a spherical shape, and a zeta potential of -48.8 mV, were evaluated for their anticancer properties against MCF-7 cell lines (Figure 8). Notably, the IC₅₀ value for these biosynthesized CuO-NPs against MCF-7 cells was recorded at 120 µg/mL [40]. This suggests that the CuO-NPs derived from *I. linnaei* Ali exhibited enhanced toxicity towards the MCF-7 cell line compared to the CuO-NPs biosynthesized from *Dillenia indica*. The CuO NPs demonstrated their special anticancer effects via various signaling routes, such as antioxidant activity, apoptosis, ROS generation, autophagy, and cell cycle arrest [41].

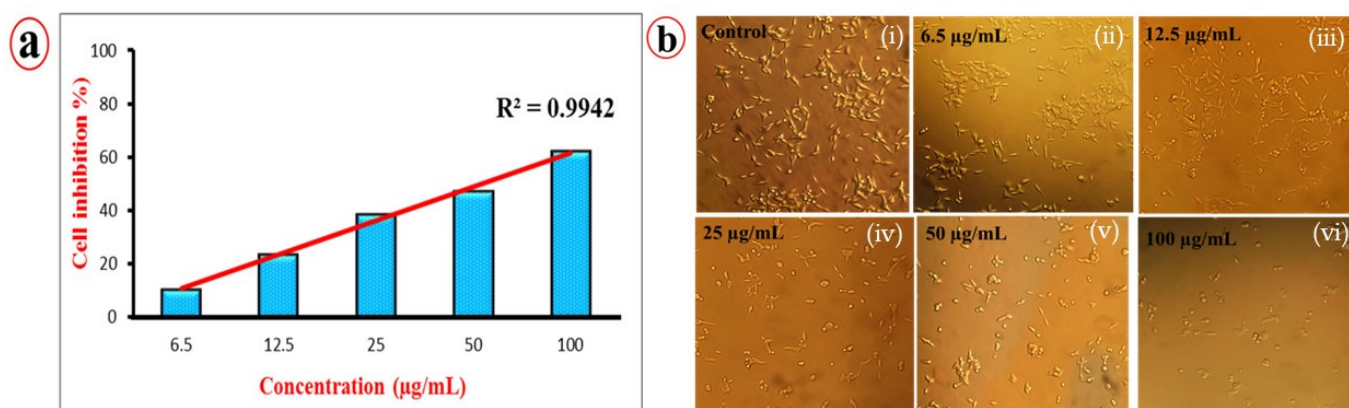


Figure 8. (a) % of cell inhibition toward MCF-7. (b) Confocal microscopy images of control and CuO-NPs against breast cancer cell line MCF-7; (i) control, (ii) 6.5 µg/mL, (iii) 12.5 µg/mL, (iv) 25 µg/mL, (v) 50 µg/mL, and (vi) 100 µg/mL (under 100 µm).

The cytotoxic effect of CuO-NPs on cancer cells can be attributed to a myriad of mechanisms. Several studies have documented that CuO-NPs exert anticancer effects through several cellular pathways, including the induction of oxidative stress, apoptosis, ROS generation, autophagy, and cell cycle arrest. Such multi-faceted modes of action make CuO-NPs potential candidates for targeted cancer therapeutics, highlighting the significance of ongoing research in this domain.

3. Materials and Methods

3.1. Collection and Substantiation of Plants

Indigofera linnaei Ali Plant samples were collected from the Biodiversity Garden located at Periyar University, Salem, India (11.7188° N, 78.0779° E). Plants were identified using a herbarium located at the Department of Botany, Periyar University, Tamil Nadu, India

(Herbarium No: PU/BOT/AVN.657). The whole plant leaves were washed several times with sterile deionized water and dried for 15 days in the shade at room temperature. Subsequently, the completely dried plants were ground into a fine powder and stored for further experiments.

3.2. Preparation of CuO NPs Using Aqueous Extract of *Indigofera tinctoria* Ali Plants

Copper Sulfate ($\text{CuSO}_4 \cdot 5\text{H}_2\text{O}$) solution was prepared in deionized water and stored in brown bottles. One gram of plant powder was dissolved in 100 mL of deionized water and heated at 60 °C for 45 min. After cooling to room temperature, the plant extract was filtered through Whatman No. 1 filter paper. Approximately 80 mL of the plant extract was mixed with 20 mL of 10% (*w/v*) $\text{CuSO}_4 \cdot 5\text{H}_2\text{O}$ solution and boiled at 80 °C on a hot plate under stirring conditions to obtain the green-colored final product. The final product was stored in a hot air oven and heated at 400 °C for 2 h using a furnace. Finally, a black precipitate was obtained and ground using a mortar and pestle for further analyses [42].

3.3. Characterization of Synthesized Copper Nanoparticles

The initial characterization of copper nanoparticles was carried out using ultraviolet-visible (UV-Vis) spectroscopy (model: UV- 1800, Make: Shimadzu, Kyoto, Japan) in a scanning wavelength range of 200–800 nm as a preliminary confirmation of copper ion reduction. FT-IR (Shimadzu IR Spirit, Kyoto, Japan) was performed in the range from 500 to 5000 cm^{-1} . This analysis was helpful for detecting the biomolecules of the whole-plant *I. tinctoria* Ali extract in the aqueous extract of plants responsible for the formation of CuO-NPs. Scanning electron microscopy combined (ZEISS, Gemini SEM 360, Jena, Germany) with EDX (Carl Zeiss Microscopy Germany, model: EVO 18) was used to identify the surface morphology, size, and elemental composition of *I. tinctoria* Ali whole-plant-extract-mediated CuO NPs.

3.4. Evaluation of the Antibacterial Activity Using Agar Well Plate Method

The antibacterial activities of CuO-NPs were evaluated, using an Agar well plate method, against four pathogenic bacteria, namely, *Staphylococcus aureus* (ATCC 25923), *Enterococcus faecalis* (ATCC 19433), *Escherichia coli* (ATCC 25922), and *Pseudomonas aeruginosa* (ATCC 25668), procured from the Applied Microbiology Laboratory, Department of Microbiology, Periyar University, Salem, India. Subsequently, 18 h bacterial culture was prepared in nutrient broth. The Muller Hinton agar (MHA) medium was prepared and poured into Petri dishes, and once solidified, an even spread of bacterial cultures was swabbed on the MHA plates with a sterile cotton swab; 6 mm wells were created on the MHA plates using a sterile cork borer. A stock solution of CuO-NPs was prepared by dissolving 500 mg of CuO-NPs in DMSO to achieve a concentration of 500 mg/mL. From the 500 mg/mL stock, 150.00, 300.00, 450.00, and 600.00 $\mu\text{g}/\text{mL}$ concentrations were prepared. The exact volume (30 μL) required to achieve these concentrations was determined using the $C1V1 = C2V2$ formula. A total of 30 μL of each prepared CuO-NP concentration was transferred into each well on the MHA plates. Amoxicillin (AMX) and DMSO served as positive and negative controls, respectively. Afterward, all plates were incubated at 37 °C for 24 h. Following incubation, the inhibition zones that formed around the wells were measured. The assay was performed in triplicate to ensure reproducibility.

3.5. Determination of Minimum Inhibitory Concentration (MIC)

The same four pathogenic bacterial strains were used for MIC determination. A bacterial suspension was prepared in a sterile nutrient broth to attain a 0.5 McFarland standard (1×10^8 CFU/mL). A stock solution of CuO-NPs was prepared by dissolving 500 mg of CuO-NPs in DMSO to obtain a concentration of 500 mg/mL. Two-fold serial dilutions of CuO-NPs were prepared in Mueller–Hinton broth (MHB) in sterile test tubes. The highest concentration (600 $\mu\text{g}/\text{mL}$) was serially diluted to attain lower concentration (150 $\mu\text{g}/\text{mL}$). To each tube containing the CuO-NPs dilutions, equal volumes of bacterial

suspension (100 µL) were added. A smooth control tube (MHB + bacterial suspension without CuO-NPs) and sterility control tube (MHB + CuO-NPs without bacterial strains) were also prepared. All tubes were labelled and incubated at 37 °C for 24 h. Following incubation, each tube was examined for turbidity (visible growth). The MIC was defined as the lowest concentration of CuO-NPs in the test tube that showed no visible bacterial growth compared with the control. The OD value was determined using a UV-Vis spectrophotometer (model: UV-1800, Make: Shimadzu, Kyoto, Japan). The experiment was conducted in triplicate for accuracy.

3.6. Larvicidal Activity

Culex quinquefasciatus mosquito larvae were bred under laboratory conditions. The larvae were reared in plastic trays containing dechlorinated water and fed regularly until the experiment was performed. Different concentrations of CuO-NPs were prepared, ranging from 20 to 100 µg/mL. The 4th-instar larvae were used in the experiment. Individual containers were filled with 49 mL of dechlorinated water, and 1 mL of each concentration was added to the respective container and labeled. Subsequently, 10 larvae were introduced into each container at each concentration in all experiments. The experiments were conducted in standard climatic conditions, such as 12 h of light and 12 h of darkness, at 28 ± 1 °C. This experiment was undisturbed and observed for 24 h for a total period of 48 h, after which dead larvae were recorded. The mortality rate at each concentration was calculated using the following formula:

$$\% \text{ of mortality} = \left(\frac{\text{number of dead larvae}}{\text{total larvae introduced}} \right) \times 100$$

3.7. Anticancer Activity Determined via MTT Assay

The human breast cancer cell line (MCF-7) was purchased from the National Centre for Cell Science, Pune. The cell line was grown in Eagle's essential media with 10% fetal bovine serum (FBS) and 1% streptomycin. These cells were maintained at 37 °C, with 5% carbon dioxide, 95% air, and 100% relative humidity. The MTT (3-(4,5-dimethylthiazol-2-yl)-diphenyl tetrazolium bromide) assay was carried out to determine the cytotoxicity of *I. linnaei* Ali-synthesized CuO NPs.

The MTT test was performed using seeded cells in 96 well plates at a density of 5000 cells per well, and the cells were left to attach for 24 h. Different concentrations of CuO-NPs (6.5, 12.5, 50.0, and 100.0 µg/mL) were prepared using DMSO and added to wells. For control wells, only DMSO, without CuO-NPs, was added. The plates were then incubated for a specific period of 24–48 h. After incubation, the media were removed from each well. Thereafter, 100 µL of fresh medium and 10 µL of MTT solution (5 mg/mL in PBS) were added to each well. The plates were incubated for another 4 h at 37 °C. Afterward, the medium was carefully withdrawn without disturbing the formazan crystals. A total of 100 µL of DMSO was added to each well to dissolve the formazan crystals. The absorbance was measured using a microplate reader at 560 nm. The percentage of cells that survived and the estimated concentration of CuO-NPs necessary to kill 50% of cancer cells were compared to those of the control. Later, the treated MCF-7 cell line was analyzed using confocal microscopic observation with 100 µm magnification (FV4000, Confocal Microscopy, Olympus, Bartlett, TN, USA). The percentage of cell inhibition was measured by plotting a bar graph with the concentration of CuO-NPs on the Y-axis and cell inhibition (%) on the X-axis. The IC₅₀ value, which represents the concentration of CuO-NPs required to inhibit the experiments at 50% cell viability, was determined from the dose–response curve. A concentration with a lower IC₅₀ value was indicative of higher anticancer activity. The experiment was conducted three times, and statistical analysis was performed using One-Way ANOVA to interpret significant differences [43,44].

$$\text{Cell viability}(\%) = \left(\frac{\text{Absorbance of treated cells}}{\text{Absorbance of control}} \right) \times 100$$

4. Conclusions

The current study demonstrates the potential of the leaf extract from the Indian medicinal plant *I. linnaei* Ali in the green synthesis of CuO-NPs. The effective formation of CuO-NPs was evident from the UV-vis results, which presented distinctive λ -max peaks at 267 and 337 nm. FT-IR was used to determine the presence of specific functional groups in the synthesized CuO-NPs. The crystalline nature of the synthesized CuO-NPs was confirmed via XRD. Additionally, SEM and EDX analyses revealed the morphology and elemental composition of the nanoparticles. A remarkable aspect of our research is the biomedical potential of the green-synthesized CuO-NPs, which exhibited significant antibacterial competence against pathogenic bacteria, including *Staphylococcus aureus*, *Pseudomonas aeruginosa*, *Escherichia coli*, and *Enterococcus faecalis*. Regarding vector control, these CuO-NPs demonstrated promising insecticidal activity, especially against the *Culex quinquefasciatus* larvae, and showed low LC₅₀ (55.716 μ g/mL) and LC₉₀ (123.657 μ g/mL) values. Furthermore, the potential therapeutic efficacy of these nanoparticles was evident from their selective cytotoxicity towards the human breast cancer cell line (LC₅₀—63.13 μ g/mL), suggesting their potential as a candidate for cancer therapy. Overall, the results from this study not only uphold the efficacious use of *I. linnaei* Ali-mediated nanoparticle synthesis but also highlight the multifaceted biomedical applications of CuO-NPs, laying a basis for further research and potential therapeutic interventions in the medical field.

Author Contributions: Conceptualization, N.P. and S.V.; methodology, S.V.; software, N.D., S.R.K. and M.S.S.; validation, N.D., S.R.K. and M.S.S.; formal analysis, M.R.S. and B.S.; investigation, N.P. and S.V.; resources, S.V. and M.R.S.; data curation, N.P., M.R.S. and B.S.; writing—original draft preparation, N.P., S.V. and M.R.S.; writing—review and editing, N.D., S.R.K. and M.S.S.; visualization, S.V.; supervision, S.V.; project administration, S.V.; funding acquisition, M.R.S. All authors have read and agreed to the published version of the manuscript.

Funding: Researchers Supporting Project number (RSPD2023R665), King Saud University, Riyadh, Saudi Arabia.

Data Availability Statement: Data contained within the article.

Acknowledgments: The authors acknowledge the funding from Researchers Supporting Project number (RSPD2023R665), King Saud University, Riyadh, Saudi Arabia.

Conflicts of Interest: The authors declare no conflict of interest.

References

1. Bouafia, A.; Meneceur, S.; Chami, S.; Laouini, S.E.; Daoudi, H.; Legmairi, S.; Mohammed Mohammed, H.A.; Aoun, N.; Mena, F. Removal of hydrocarbons and heavy metals from petroleum water by modern green nanotechnology methods. *Sci. Rep.* **2023**, *13*, 5637. [[CrossRef](#)] [[PubMed](#)]
2. Gu, J.; Chen, F.; Zheng, Z.; Bi, L.; Morovvati, H.; Goorani, S. Novel green formulation of copper nanoparticles by *Foeniculum vulgare*: Chemical characterization and determination of cytotoxicity, anti-human lung cancer and antioxidant effects. *Inorg. Chem. Commun.* **2023**, *150*, 110442. [[CrossRef](#)]
3. Dejen, K.D.; Kibret, D.Y.; Mengesha, T.H.; Bekele, E.T.; Tedla, A.; Bafa, T.A.; Derib, F.T. Green synthesis and characterisation of silver nanoparticles from leaf and bark extract of *Croton macrostachyus* for antibacterial activity. *Mater. Technol.* **2023**, *38*, 2164647. [[CrossRef](#)]
4. Prakash, M.; Kavitha, H.P.; Abinaya, S.; Vennila, J.P.; Lohita, D. Green synthesis of bismuth based nanoparticles and its applications—A review. *Sustain. Chem. Pharm.* **2022**, *25*, 100547. [[CrossRef](#)]
5. Nihunya, L.N.; Mbakop, S.; Makgabutlane, B.; Matlou, G.; Mhlanga, S.; Richards, H. Fungal synthesis of copper nanoparticles and their applications in agri-food, environmental, and biomedical sectors. In *Fungal Cell Factories for Sustainable Nanomaterials Productions and Agricultural Applications*; Elsevier: Amsterdam, The Netherlands, 2023; pp. 91–114.
6. Abed, A.S.; Khalaf, Y.H.; Mohammed, A.M. Green synthesis of gold nanoparticles as an effective opportunity for cancer treatment. *Results Chem.* **2023**, *5*, 100848. [[CrossRef](#)]
7. Gemin, L.G.; de Lara, G.B.; Mógor, Á.F.; Mazaro, S.M.; Sant’Anna-Santos, B.F.; Mógor, G.; Amatussi, J.D.O.; Cordeiro, E.C.N.; Marques, H.M.C. Polysaccharides combined to copper and magnesium improve tomato growth, yield, anti-oxidant and plant defense enzymes. *Sci. Hortic.* **2023**, *310*, 111758. [[CrossRef](#)]
8. Naz, S.; Gul, A.; Zia, M.; Javed, R. Synthesis, biomedical applications, and toxicity of CuO nanoparticles. *Appl. Microbiol. Biotechnol.* **2023**, *107*, 1039–1061. [[CrossRef](#)]

9. Sukumar, S.; Rudrasenan, A.; Padmanabhan Nambiar, D. Green-synthesized rice-shaped copper oxide nanoparticles using *Caesalpinia bonducella* seed extract and their applications. *ACS Omega* **2020**, *5*, 1040–1051. [[CrossRef](#)]
10. Siddiqui, V.U.; Ansari, A.; Chauhan, R.; Siddiqi, W.A. Green synthesis of copper oxide (CuO) nanoparticles by *Punica granatum* peel extract. *Mater. Today Proc.* **2021**, *36*, 751–755. [[CrossRef](#)]
11. Ramadhan, V.; Ni'Mah, Y.; Yanuar, E.; Suprpto, S. Synthesis of copper nanoparticles using *Ocimum tenuiflorum* leaf extract as capping Agent. *AIP Conf. Proc.* **2019**, *2202*, 020067.
12. Kolahalam, L.A.; Prasad, K.; Krishna, P.M.; Supraja, N.; Shanmugan, S. The exploration of bio-inspired copper oxide nanoparticles: Synthesis, characterization and in-vitro biological investigations. *Heliyon* **2022**, *8*, e09726. [[CrossRef](#)] [[PubMed](#)]
13. Khani, R.; Roostaei, B.; Bagherzade, G.; Moudi, M. Green synthesis of copper nanoparticles by fruit extract of *Ziziphus spina-christi* (L.) Willd.: Application for adsorption of triphenylmethane dye and antibacterial assay. *J. Mol. Liq.* **2018**, *255*, 541–549. [[CrossRef](#)]
14. Cuong, H.N.; Pansambal, S.; Ghotekar, S.; Oza, R.; Hai, N.T.T.; Viet, N.M.; Nguyen, V.-H. New frontiers in the plant extract mediated biosynthesis of copper oxide (CuO) nanoparticles and their potential applications: A review. *Environ. Res.* **2022**, *203*, 111858. [[CrossRef](#)] [[PubMed](#)]
15. Verma, N.; Kumar, N. Synthesis and biomedical applications of copper oxide nanoparticles: An expanding horizon. *ACS Biomater. Sci. Eng.* **2019**, *5*, 1170–1188. [[CrossRef](#)] [[PubMed](#)]
16. Adil, S.F.; Assal, M.E.; Khan, M.; Al-Warthan, A.; Siddiqui, M.R.H.; Liz-Marzán, L.M. Biogenic synthesis of metallic nanoparticles and prospects toward green chemistry. *Dalton Trans.* **2015**, *44*, 9709–9717. [[CrossRef](#)] [[PubMed](#)]
17. Mohamed, E.A. Green synthesis of copper & copper oxide nanoparticles using the extract of seedless dates. *Heliyon* **2020**, *6*, e03123. [[PubMed](#)]
18. Rehana, D.; Mahendiran, D.; Kumar, R.S.; Rahiman, A.K. Evaluation of antioxidant and anticancer activity of copper oxide nanoparticles synthesized using medicinally important plant extracts. *Biomed. Pharmacother.* **2017**, *89*, 1067–1077. [[CrossRef](#)] [[PubMed](#)]
19. Akintelu, S.A.; Folorunso, A.S.; Folorunso, F.A.; Oyebamiji, A.K. Green synthesis of copper oxide nanoparticles for biomedical application and environmental remediation. *Heliyon* **2020**, *6*, e04508. [[CrossRef](#)]
20. Kumar, R.S.; Raj Kapoor, B.; Perumal, P. Antitumor and cytotoxic activities of methanol extract of *Indigofera linnaei* Ali. *Asian Pac. J. Cancer Prev.* **2011**, *12*, 613–618.
21. Kumar, R.S.; Raj Kapoor, B.; Perumal, P.; Kumar, S.V.; Geetha, A.S. Beneficial effects of methanolic extract of *Indigofera linnaei* Ali on the inflammatory and nociceptive responses in rodent models. *Braz. J. Pharm. Sci.* **2016**, *52*, 113–123. [[CrossRef](#)]
22. Kumar, R.S.; Kumar, S.V.; Raj Kapoor, B.; Pravin, N.; Mahendiran, D. Chemopreventive effect of *Indigofera linnaei* extract against diethylnitrosamine induced hepatocarcinogenesis in rats. *J. Appl. Pharm. Sci.* **2016**, *6*, 199–209. [[CrossRef](#)]
23. Nzilu, D.M.; Madivoli, E.S.; Makhanu, D.S.; Wanakai, S.I.; Kiprono, G.K.; Kareru, P.G. Green synthesis of copper oxide nanoparticles and its efficiency in degradation of rifampicin antibiotic. *Sci. Rep.* **2023**, *13*, 14030. [[CrossRef](#)] [[PubMed](#)]
24. Karuppanan, S.K.; Ramalingam, R.; Khalith, S.M.; Dowlath, M.J.H.; Raiyaan, G.D.; Arunachalam, K.D. Characterization, antibacterial and photocatalytic evaluation of green synthesized copper oxide nanoparticles. *Biocatal. Agric. Biotechnol.* **2021**, *31*, 101904. [[CrossRef](#)]
25. Manasa, D.; Chandrashekar, K.; Kumar, D.M.; Niranjana, M.; Navada, K.M. *Mussaenda frondosa* L. mediated facile green synthesis of copper oxide nanoparticles—characterization, photocatalytic and their biological investigations. *Arab. J. Chem.* **2021**, *14*, 103184. [[CrossRef](#)]
26. Alhalili, Z. Green synthesis of copper oxide nanoparticles CuO NPs from *Eucalyptus Globoulus* leaf extract: Adsorption and design of experiments. *Arab. J. Chem.* **2022**, *15*, 103739. [[CrossRef](#)]
27. Jayasimha, H.; Chandrappa, K.; Sanaulla, P.; Dileepkumar, V. Green synthesis of CuO nanoparticles: A promising material for photocatalysis and electrochemical sensor. *Sens. Int.* **2023**, *7*, 100254. [[CrossRef](#)]
28. Din, M.I.; Arshad, F.; Rani, A.; Aihetasham, A.; Mukhtar, M.; Mehmood, H. Single step green synthesis of stable copper oxide nanoparticles as efficient photo catalyst material. *Biomed. Mater.* **2017**, *9*, 41–48.
29. Thiruvengadam, M.; Chung, I.-M.; Gomathi, T.; Ansari, M.A.; Gopiesh Khanna, V.; Babu, V.; Rajakumar, G. Synthesis, characterization and pharmacological potential of green synthesized copper nanoparticles. *Bioprocess Biosyst. Eng.* **2019**, *42*, 1769–1777. [[CrossRef](#)]
30. Holzwarth, U.; Gibson, N. The Scherrer equation versus the 'Debye-Scherrer equation'. *Nat. Nanotechnol.* **2011**, *6*, 534. [[CrossRef](#)]
31. Tamuly, C.; Saikia, I.; Hazarika, M.; Das, M.R. Reduction of aromatic nitro compounds catalyzed by biogenic CuO nanoparticles. *RSC Adv.* **2014**, *4*, 53229–53236. [[CrossRef](#)]
32. Sharma, P.; Pant, S.; Poonia, P.; Kumari, S.; Dave, V.; Sharma, S. Green synthesis of colloidal copper nanoparticles capped with *Tinospora cordifolia* and its application in catalytic degradation in textile dye: An ecologically sound approach. *J. Inorg. Organomet. Polym. Mater.* **2018**, *28*, 2463–2472. [[CrossRef](#)]
33. Ali, M.; Ijaz, M.; Ikram, M.; Ul-Hamid, A.; Avais, M.; Anjum, A.A. Biogenic synthesis, characterization and antibacterial potential evaluation of copper oxide nanoparticles against *Escherichia coli*. *Nanoscale Res. Lett.* **2021**, *16*, 148. [[CrossRef](#)] [[PubMed](#)]
34. Wu, S.; Rajeshkumar, S.; Madasamy, M.; Mahendran, V. Green synthesis of copper nanoparticles using *Cissus vitiginea* and its antioxidant and antibacterial activity against urinary tract infection pathogens. *Artif. Cells Nanomed. Biotechnol.* **2020**, *48*, 1153–1158. [[CrossRef](#)] [[PubMed](#)]

35. Ssekatawa, K.; Byarugaba, D.K.; Angwe, M.K.; Wampande, E.M.; Ejobi, F.; Nxumalo, E.; Maaza, M.; Sackey, J.; Kirabira, J.B. Phyto-mediated copper oxide nanoparticles for antibacterial, antioxidant and photocatalytic performances. *Front. Bioeng. Biotechnol.* **2022**, *10*, 820218. [[CrossRef](#)]
36. Anduaem, W.W.; Sabir, F.K.; Mohammed, E.T.; Belay, H.H.; Gonfa, B.A. Synthesis of copper oxide nanoparticles using plant leaf extract of *Catha edulis* and its antibacterial activity. *J. Nanotechnol.* **2020**, *2020*, 2932434. [[CrossRef](#)]
37. Vinothkanna, A.; Mathivanan, K.; Ananth, S.; Ma, Y.; Sekar, S. Biosynthesis of copper oxide nanoparticles using *Rubia cordifolia* bark extract: Characterization, antibacterial, antioxidant, larvicidal and photocatalytic activities. *Environ. Sci. Pollut. Res.* **2023**, *30*, 42563–42574. [[CrossRef](#)]
38. Rajagopal, G.; Nivetha, A.; Sundar, M.; Panneerselvam, T.; Murugesan, S.; Parasuraman, P.; Kumar, S.; Ilango, S.; Kunjiappan, S. Mixed phytochemicals mediated synthesis of copper nanoparticles for anticancer and larvicidal applications. *Heliyon* **2021**, *7*, e07360. [[CrossRef](#)]
39. Tahir, A.; Quispe, C.; Herrera-Bravo, J.; Iqbal, H.; Anum, F.; Javed, Z.; Sehar, A.; Sharifi-Rad, J. Green synthesis, characterization and antibacterial, antifungal, larvicidal and anti-termite activities of copper nanoparticles derived from *Grewia asiatica* L. *Bull. Natl. Res. Cent.* **2022**, *46*, 188. [[CrossRef](#)]
40. Mohanta, L.; Jena, B.S. One-pot facile biosynthesis of copper nanoparticles using *Dillenia indica* L. bark extract for in vitro anticancer activity against human lung and breast cancer cell lines. *Res. Sq.* **2022**. [[CrossRef](#)]
41. Letchumanan, D.; Sok, S.P.; Ibrahim, S.; Nagoor, N.H.; Arshad, N.M. Plant-based biosynthesis of copper/copper oxide nanoparticles: An update on their applications in biomedicine, mechanisms, and toxicity. *Biomolecules* **2021**, *11*, 564. [[CrossRef](#)]
42. Yasin, A.; Fatima, U.; Shahid, S.; Mansoor, S.; Inam, H.; Javed, M.; Iqbal, S.; Alrbyawi, H.; Somaily, H.H.; Pashameah, R.A. Fabrication of copper oxide nanoparticles using passiflora edulis extract for the estimation of antioxidant potential and photocatalytic methylene blue dye degradation. *Agronomy* **2022**, *12*, 2315. [[CrossRef](#)]
43. Mosmann, T. Rapid colorimetric assay for cellular growth and survival: Application to proliferation and cytotoxicity assays. *J. Immunol. Methods* **1983**, *65*, 55–63. [[CrossRef](#)] [[PubMed](#)]
44. Monks, A.; Scudiero, D.; Skehan, P.; Shoemaker, R.; Paull, K.; Vistica, D.; Hose, C.; Langley, J.; Cronise, P.; Vaigro-Wolff, A. Feasibility of a high-flux anticancer drug screen using a diverse panel of cultured human tumor cell lines. *JNCI J. Natl. Cancer Inst.* **1991**, *83*, 757–766. [[CrossRef](#)] [[PubMed](#)]

Disclaimer/Publisher's Note: The statements, opinions and data contained in all publications are solely those of the individual author(s) and contributor(s) and not of MDPI and/or the editor(s). MDPI and/or the editor(s) disclaim responsibility for any injury to people or property resulting from any ideas, methods, instructions or products referred to in the content.